Molecular Vision 2023; 29:68-86 <http://www.molvis.org/molvis/v29/68>
Received 1 September 2022 | Accepted 18 May 2023 | Published 20 May 2023

Corneal epithelial basement membrane assembly is mediated by epithelial cells in coordination with corneal fibroblasts during wound healing

Thomas Michael Shiju, Lycia Pedral Sampaio, Guilherme S. L. Hilgert, Steven E. Wilson

Cole Eye Institute, Cleveland Clinic, Cleveland, Ohio

Purpose: To understand which cell types, either alone or in combination, contribute to the assembly of the epithelial basement membrane (BM) during corneal wound healing.

Methods: A 3D corneal organotypic model and an in situ rabbit photorefractive keratectomy (PRK) model were used in this study. The 3D corneal organotypic model was established by culturing the rabbit corneal epithelial cells with either corneal fibroblasts or myofibroblasts embedded in collagen type I for 18 days. Corneal fibroblasts were isolated from fresh rabbit corneas, and the myofibroblasts were derived either directly from bone marrow or differentiated from corneal fibroblasts. Immunocytochemistry for alpha-smooth muscle actin (SMA), vimentin, desmin, and vinculin markers confirmed well-differentiated myofibroblasts. Immunohistochemistry was performed in cryofixed sections for BM markers, including laminin alpha-5, laminin beta-3, perlecan, nidogen-1, and collagen type IV. Specimens were also examined with transmission electron microscopy (TEM). Corneas were collected from rabbits after −3 diopter (D) PRK at different time points after surgery, with four corneas at each time point in each group. Cryofixed corneal sections were stained for vimentin, alpha-SMA, and nidogen-1.

Results: The formation of an epithelial BM with expression of laminin alpha-5, laminin beta-3, perlecan, nidogen-1, and collagen IV was observed at the interface between the corneal epithelial cells and corneal fibroblasts. TEM images further confirmed the presence of epithelial BM in organotypic cultures of epithelial cells and corneal fibroblasts. No epithelial BM was observed in cultures of corneal epithelial cells and myofibroblasts (cornea or bone marrow derived), corneal epithelial cells alone, or corneal fibroblasts alone. In rabbit corneas after −3D PRK, a strong association was observed between the regenerating epithelial BM and the presence of corneal fibroblasts at the site of epithelial BM generation.

Conclusions: The corneal epithelial BM assembly is mediated by epithelial cells in coordination with corneal fibroblasts during wound healing.

Epithelial-stromal interactions are established at an early stage of tissue development and play an important role in maintaining tissue integrity and homeostasis [1-3]. The basement membrane (BM) is a specialized thin sheet that acts as a bridge anchoring the multi-layered epithelium to the underlying stroma [4] and supports epithelial cell adhesion, migration, and differentiation [5-8]. The sheet-like structure is derived from two independent polymeric networks—laminin and collagen type IV—interlinked by other extracellular matrix (ECM) proteins, such as nidogen/entacin and perlecan [9,10]. Apart from physical support, the epithelial BM serves many important functions in corneal physiology [11]. For example, one of the most important functions of the epithelial BM is to bidirectionally modulate the availability of cytokines and growth factors that serve critical functions in corneal homeostasis and the response to injury. Thus, the epithelial BM modulates the bioavailability of growth factors, such as transforming growth factor (TGF) beta-1 and beta-2 and platelet-derived growth factor (PDGF), which are present in tears and produced by the corneal epithelium to regulate myofibroblast generation from corneal fibroblasts and bone marrow-derived fibrocytes in response to corneal injury [11-17]. The epithelial BM also regulates the delivery of keratocyte/corneal fibroblast-produced hepatocyte growth factor (HGF) and keratinocyte growth factor (KGF), which modulate the motility, proliferation, differentiation, and apoptosis of the overlying corneal epithelial cells [11,18-22].

The normal unwounded corneal stroma is populated by relatively quiescent keratocytes that secrete ECM proteins and enzymes to maintain ECM homeostasis within the stroma [23]. After an injury (e.g., trauma, infection, or surgery), keratocytes transition to an active repair phenotype (corneal fibroblasts), which may further trans-differentiate into myofibroblasts if exposed to adequate and ongoing levels of TGF beta-1 and/or TGF beta-2 [24-26]. In addition,

Correspondence to: Steven E. Wilson, Cole Eye Institute, I-32, Cleveland Clinic, 9500 Euclid Ave, Cleveland, OH; Phone: (216) 444 3871; FAX: (216) 445 8475; email: wilsons4@ccf.org

bone marrow-derived fibrocytes that infiltrate into the injured tissue also undergo TGF beta-driven differentiation into myofibroblasts in the corneal stroma [16,27]. Thus, the injured corneal stroma is occupied by a diverse population of cells that include at least two progenitor cells to myofibroblasts as well as other infiltrating cells such as monocytes, macrophages, polymorphonuclear cells, and lymphocytes.

Myofibroblasts that develop in the cornea function in the contraction of wounds and ECM deposition to maintain corneal integrity after injury. This role also produces opacity that interferes with the primary function of the cornea in vision. If the epithelial BM is not fully regenerated, the ongoing passage of growth factors from the tears and epithelium, such as TGF beta-1 and TGF beta-2 as well as other cytokines and growth factors, into the stroma promotes excessive myofibroblast differentiation and their persistence, eventually producing longstanding stromal fibrosis and corneal opacity [17,28].

Thus, epithelial BM regeneration has a critical role in modulating the response to injury and a return to normal corneal function. Studies in other tissues have suggested that there is coordination between epithelial cells and underlying stromal cells in the regeneration of BMs after injury [29-34]. However, uncertainty remains regarding whether similar coordination between different cells occurs during corneal epithelial BM regeneration. This study was designed to explore the cells responsible for corneal epithelial BM assembly using 3D organotypic cultures and rabbit in situ injury models.

METHODS

Primary culture of corneal fibroblasts and myofibroblasts: Corneal fibroblast isolation and myofibroblast differentiation were performed based on the method developed by McKay et al. [35]. Briefly, rabbit corneas (Cat. #41,209-2; Pel-Freez Biologicals, Rogers, AR) were procured and processed on the day of arrival approximately 24 h after enucleation. The corneas were punched centrally using a 9-mm trephine in a sterile Petri dish containing phosphate buffered saline (PBS) with 1× penicillin-streptomycin antibiotic solution (Cat. #30–002; Corning, Tewksbury, MA). The epithelial and endothelial layer, along with the BMs, were removed under a dissection microscope using a scalpel blade. The corneal stroma was cut into ~2-mm^2 pieces and incubated overnight at 37 °C in a solution with 50 mg of collagenase (Cat. #C0130–1G; Sigma-Aldrich, Burlington, MA) and 25 mg of hyaluronidase (Cat. #H3884–100MG; Sigma-Aldrich) dissolved in 50 ml of Hanks balanced salt solution (HBSS) containing 0.5-mM magnesium chloride ($MgCl_2$) and 1.26-mM calcium chloride ($CaCl_2$). The tissue homogenate was centrifuged at 100 g for 10 min at room temperature. The supernatant was discarded, and the pellet was resuspended in 10 ml of 1× HBSS solution and again centrifuged with the same settings. The stromal cell pellet was cultured in a corneal fibroblast medium Eagle's minimal essential medium (EMEM, 10% FBS; Cat. #1600004; Thermo Fisher Scientific, Grand Island, NY), 1× penicillin-streptomycin solution (Cat. #30–002; Corning), and 40 ng/ml of recombinant fibroblast growth factor-basic (Cat. #100–18B; Peprotech, Cranbury, NJ). The cells were incubated in T-25 flasks (Corning) at 37°C and 5% carbon dioxide (CO_2). The medium was changed every other day until the cells reached 70% confluency. Once the desired confluency was reached, 50% of the cells were incubated in a myofibroblast differentiation medium (MEM, 10% FBS, 1× penicillin-streptomycin, 20 ng/ml of TGF β-1; Cat. #100–21; Peprotech), and the remaining 50% were maintained in a fibroblast medium for use as corneal fibroblasts (Figure 1A) in organotypic cultures. The cells were incubated in TGF β-1 for 7 to 10 days to achieve complete differentiation into myofibroblasts (Figure 1A). The myofibroblast phenotype was confirmed by performing immunocytochemistry (ICC) for the myofibroblast markers alpha-smooth muscle actin (SMA), vimentin, vinculin, and desmin (Figure 1B). Myofibroblasts were then used for the preparation of organotypic cultures.

Bone marrow-derived myofibroblasts (Figure 1B) were also cultured from rabbits using a previously described method [36]. These myofibroblasts were used in organotypic cultures with rabbit corneal epithelial cells either alone or in different proportions with corneal myofibroblasts.

3D organotypic cultures: The 3D corneal organotypic cultures were generated based on the skin reconstruction model developed by Li et al. [37] with minor modifications [38], and the schematic workflow for developing 3D corneal organotypic cultures is illustrated in Figure 2. The acellular layer was prepared by mixing the following reagents in ice: 0.59 ml of 10× EMEM, 50 µl of 200-mM L-glutamine, 0.6 ml of FBS (Cat. #1600004; Thermo Fisher Scientific), 120 µl of 7.5% sodium bicarbonate, and 4.6 ml of rat collagen-1 (2 mg/ml; Cat. #354249; Corning). Next, 1 ml of this mixture was added to each insert of the 6-well tissue culture trays (Cat. #3414; Corning). The acellular layer was incubated at 37 °C for 1 to 2 h until the collagen gel solidified. A change of color from straw-yellow to pink was used as an indicator for collagen gel solidification. Fibroblasts or myofibroblasts were trypsinized using 0.25% trypsin-ethylenediaminetetraacetic acid (EDTA) and neutralized with DMEM containing 10% FBS. The cell suspension was then centrifuged at 180 g for 7

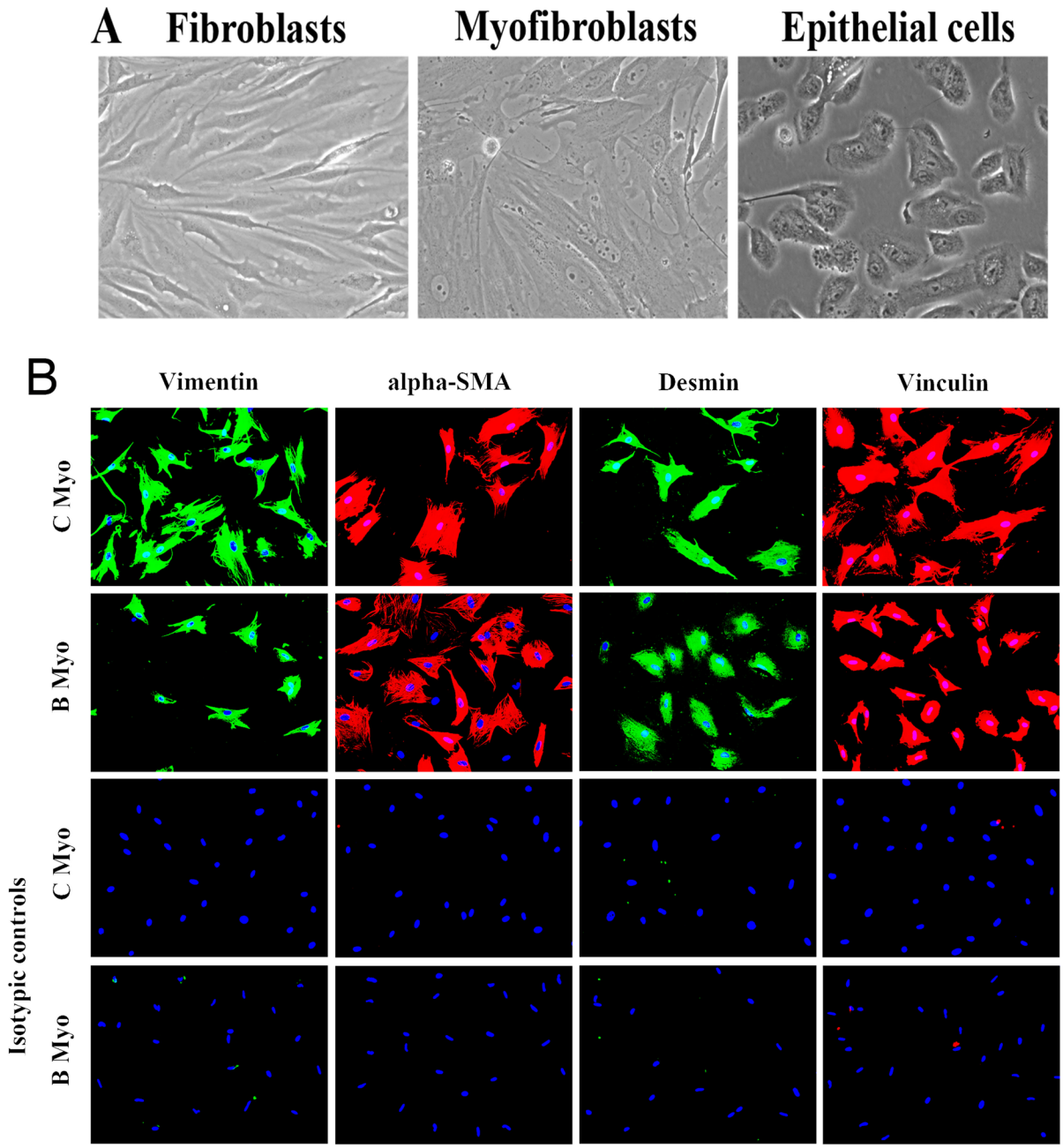

Figure 1. Confirmation of cell morphology using light microscopy and immunocytochemistry **A**: Phase-contrast microscopy of rabbit corneal fibroblasts, myofibroblasts, and epithelial cells. Mag.:100×. **B**: Immunocytochemistry (ICC) for myofibroblast markers in cornea- and bone marrow-derived myofibroblasts. Myofibroblasts cultured in transforming growth factor (TGF) beta-1 for 14 days had ICC for vimentin, alpha-smooth muscle actin (SMA), desmin, and vinculin. Both cornea- and bone marrow-derived cells expressed vimentin, alpha-SMA, desmin, and vinculin, indicating they were vimentin-alpha smooth muscle actin-desmin (VAD)-positive myofibroblasts (Chaurasia et al., 2009). ICC with the corresponding isotypic control antibodies was also performed for each marker. Blue is 4′,6-diamidino-2-phenylindole (DAPI) staining of the nuclei. Mag.: 200×.

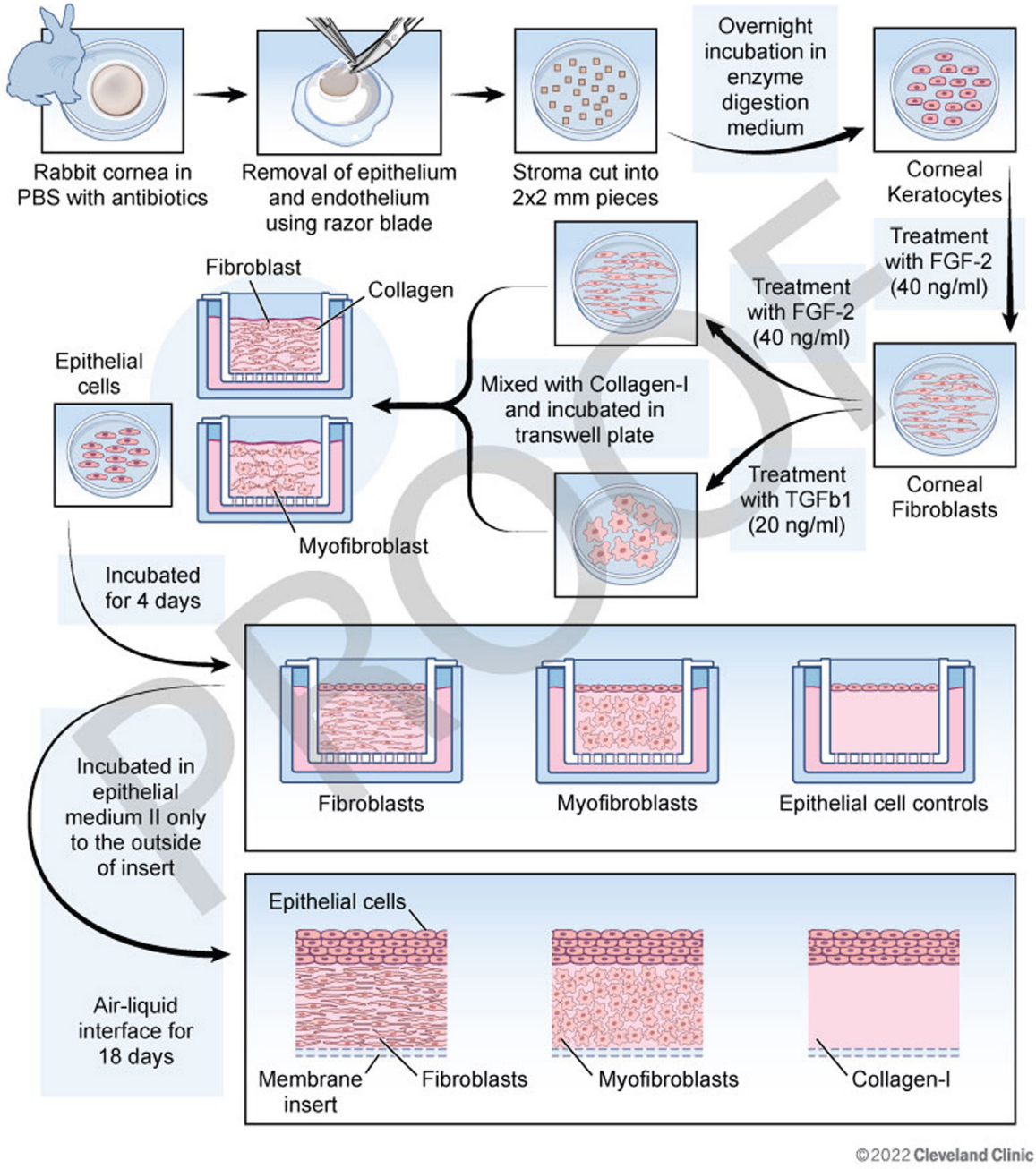

Figure 2. Schematic workflow for preparing 3D corneal organotypic cultures. Rabbit corneas were procured and processed on the day of arrival approximately 24 h after enucleation. The corneas were punched centrally using a 9-mm trephine in a sterile Petri dish containing phosphate buffered saline (PBS) with 1× penicillin-streptomycin antibiotic solution. The epithelial and endothelial layers, along with the basement membranes (BMs), were removed under a dissection microscope using a scalpel blade. The corneal stroma was cut into ~2-mm^2 pieces and incubated overnight in an enzyme digestion medium containing collagenase and hyaluronidase. The stromal cell pellet collected after a brief centrifugation contained the corneal keratocytes, which were incubated in a fibroblast medium containing 40 ng/ml of fibroblast growth factor (FGF-2). Once the desired confluency was reached, 50% of the cells were treated with a myofibroblast medium containing 20 ng/ml of TGF beta-1, and the remaining 50% were maintained in the fibroblast medium. The cells were mixed with collagen type-1 to prepare the cellular layer, which was loaded above the acellular layer and coated onto the insert of six-well Transwell plates (Corning, NY). The cellular layer was incubated undisturbed for 4 days at 37°C in 5% carbon dioxide (CO_2). On Day 5, epithelial cells procured from commercial sources were prepared as a cell suspension and added to each insert, which was then incubated for 2 days in epithelial medium I at 37°C. Subsequently, the media was removed from both the inside and outside of the insert and replaced with fresh epithelial growth medium II only to the outside of the insert. The epithelial cells were then exposed to the air–liquid interface for 18 days, and the medium was replaced every 2 days. At the end of 18 days of incubation, a 3D corneal construct with different combinations of stromal cells along with multi-layered epithelial cells was generated.

min, and the cell pellets were resuspended in their respective media at a cell count of 0.45 × 10^6 cells/ml.

The cellular layer was prepared by mixing 1.65 ml of 10× EMEM, 150 µl of 200-mM L-glutamine, 1.85 ml of FBS, 350 µl of 7.5% sodium bicarbonate, 14 ml of bovine collagen type I (2 mg/ml), and 1.5 ml of cell suspension in a 50 ml tube on ice. Next, 3 ml of the cellular layer was added above the acellular layer in each well and incubated at 37 °C and 5% CO_2 for 45 min. Once the collagen gel was solidified (indicated by a color change from straw-yellow to pink), 1 ml of cell-specific medium was added above the cellular layer, and 3 ml was added outside of the insert. The cellular layer was incubated undisturbed for 4 days at 37 °C in 5% CO_2. On Day 5, the media were removed from both the inside and outside of the insert, and the insert was incubated in a washing medium (HBSS with 1% dialyzed FBS; Cat. #A3382001; Thermo Fisher Scientific) for 1 h at 37°C. Meanwhile, the rabbit corneal epithelial cells (Figure 1A; Rb630–05; Cell Applications, San Diego, CA and N-6048; Cell Biologics, Chicago, IL) were trypsinized and resuspended at 4.1 × 10^6 cells/ml in epithelial medium I, which was a mixture of a corneal epithelial cell medium (Rb221–500; Cell Applications), 264 ng/ml of stem cell factor (Cat. #300–07; Peprotech), and 10 ng/ml of endothelin-3 (Cat. #MBS405523; MyBioSource, San Diego, CA). The wash medium was removed, and the epithelial cell growth medium was added both to the inside (1 ml) and outside (3 ml) of the insert. Finally, 100 µl of epithelial cell suspension was added to each insert and incubated for 2 days at 37 °C. Subsequently, the media were removed from both the inside and outside of the insert and replaced with fresh epithelial growth medium II (epithelial cell growth medium I + 1M $CaCl_2$) on only the outside of the insert. The epithelial cells were then exposed to the air–liquid interface for 18 days, and the medium was replaced every 2 days.

Organotypic cultures of rabbit corneal epithelial cells with bone marrow-derived myofibroblasts or mixtures of 50% cornea-derived myofibroblasts and 50% bone marrow-derived myofibroblasts were prepared using the same methods. Organotypic cultures prepared using 1) the corneal fibroblasts with collagen matrix but without epithelial cells, 2) corneal myofibroblasts with collagen matrix but without epithelial cells, and 3) epithelial cells added above the collagen matrix without fibroblast/myofibroblast served as controls.

Cryofixation of corneal organotypic culture: The media were aspirated from both the inside and outside of the insert in the culture well, and the 3D cultured construct was incubated in 4% paraformaldehyde for 1 h at room temperature. The constructs were then incubated in 50% sucrose for 2 h at 4°C followed by incubation in 2M sucrose for another 2 h at 4 °C. Finally, the corneal constructs were removed from the sucrose and placed in a mold (Cat. #62,352-24; Thermo Fisher Scientific) containing an optimal cutting temperature (OCT) freezing medium (Cat. #4583; Sakura Finetek, Torrance, CA). The molds were placed on dry ice until the OCT was frozen and were then stored at −80°C until cryo-sectioning.

Animals and surgeries: All procedures involving animals were approved by the Institutional Animal Care and Use Committee (IACUC) at the Cleveland Clinic Foundation (Cleveland, OH). All animals were treated in accordance with the tenets of the Association for Research in Vision and Ophthalmology (ARVO) Statement for the Use of Animals in Ophthalmic and Vision Research.

Twenty-four female 12- to 15-week-old New Zealand white rabbits weighing 2.5 to 3.0 kg each were included in this study. Photorefractive keratectomy (PRK) was performed as previously described [39]. Briefly, one eye of each rabbit was selected at random to have −3D moderate-injury PRK with a 6-mm diameter ablation zone using a VISX Star S4 IR excimer laser (Abbott Medical Optics, Irvine, CA). In addition, four bilateral unwounded rabbit corneas were used as controls.

Anesthesia before surgery was performed by intramuscular injection of ketamine hydrochloride (30 mg/kg) and xylazine hydrochloride (5 mg/kg) in addition to topical administration of 1% proparacaine hydrochloride ophthalmic solution (Alcon, Fort Worth, TX). After the procedure, one drop of moxifloxacin (Alcon) was applied to the PRK corneas four times a day until the epithelium closed. No corticosteroids or mitomycin C was used in this study.

Euthanasia was performed by intravenous injection of 100 mg/kg of Beuthanasia (Shering-Plough, Kenilworth, NJ) while the animals were under general anesthesia. The corneo-scleral rims of the wounded and unwounded eyes were removed with 0.12 forceps and sharp Westcott scissors (Fairfield, CT) without touching the cornea. The corneo-scleral rims were placed in the center of a 24 × 24 × 5-mm mold (Cat. #62,352-24; Thermo Fisher Scientific, Pittsburgh, PA) and immersed in the OCT compound. The corneo-scleral rim within the mold was rapidly frozen on dry ice, and the blocks were stored at −80 °C until cryo-sectioning.

Cryo-sectioning and immunohistochemistry: Transverse sections (16 µm thick) were cut from each specimen with a cryostat (HM 505M; Micron, Walldorf, Germany) and placed on 25 × 75 × 1-mm Superfrost Plus microscope slides (Cat. #12–550–15; Thermo Fisher Scientific). Slides were

maintained at −80 °C until immunohistochemistry (IHC) for epithelial BM components was performed.

Triplex IHC was performed for the epithelial BM components laminin alpha-5, perlecan, and nidogen-1. First, the slides were thawed for 5 min at room temperature and then immersed in 1 × PBS twice for 5 min. The slides were then fixed by incubating in 4% paraformaldehyde for 5 min. Slides were rinsed twice in 1× PBS solution and subsequently blocked for 1 h at room temperature with 5% donkey serum (Cat. #017–000–121; Jackson ImmunoResearch, West Grove, PA) in PBS containing 0.05% NP-40. Slides were then incubated for 90 min with three primary antibodies—chicken anti-laminin alpha-5 (H9511; a gift from Peter Yurchenco, PhD) at 1:50 dilution, mouse anti-perlecan (Cat. #sc-377219; Santa Cruz Biotechnology, Dallas, TX) at 1:50 dilution, and goat anti-nidogen-1 (Cat. #AF2570, R&D systems, Minneapolis, MN) at 1:25 dilution—in a blocking buffer. Slides were subsequently washed three times with 1× PBS and incubated for 1 h with the three corresponding secondary antibodies—donkey anti-chicken Alexa Fluor 488 (Cat. #703–605–155; Jackson ImmunoResearch, West Grove, PA), donkey anti-mouse Alexa Fluor 568 (Cat. #A10037; Thermo FisherScientific), and donkey anti-goat Alexa Fluor 680 (Cat. #A21084; Thermo Fisher Scientific)—at 1:200 dilutions at room temperature. After the slides were rinsed three times in 1× PBS, 24 × 60-mm glass coverslips (Cat. #48393–251; VWR, Radnor, PA) were mounted with Vectashield containing 4′,6-diamidino-2-phenylindole (DAPI; H-1200; Vector Laboratories, Burlingame, CA) to visualize all cell nuclei. Slides were analyzed and imaged with a Leica DM5000 microscope (Leica, Buffalo Grove, IL) equipped with a Q-imaging Retiga 4000 RV (Surrey, BC, Canada) camera and Image-Pro software (Media Cybernetics, Bethesda, MD).

Using the same methodology, duplex IHC for collagen type IV (goat anti-collagen type IV, Cat. #AB769, Sigma-Aldrich; 1:100 dilution) and mouse anti-laminin beta-3 (Cat. #NBP2–46622, Novus Biologicals, Centennial, CO; 1:100 dilution) was performed using the secondary antibodies donkey anti-mouse Alexa Fluor 488 and donkey anti-goat Alexa Fluor 568, both at 1:200 dilutions.

Triplex IHC was also performed to simultaneously detect the expression of epithelial BM markers (goat anti-nidogen-1, Cat. #AF2570; R&D systems; 1:25 dilution), mesenchymal marker vimentin (rat IgG, #Mab2105; R&D Systems; 1:100 dilution), and the myofibroblast marker alpha-SMA (mouse IgG2a, kappa, #M0851; Agilent Dako, Santa Clara, CA; 1:200 dilution) using the methods described above. Importantly, at the concentration of anti-vimentin antibody used, corneal fibroblasts and myofibroblasts were vimentin positive. However, most keratocytes express vimentin at lower levels and would not be detected in this IHC assay, even though keratocytes would be vimentin-positive with higher antibody concentrations [17,40].

Quantitation of IHC images for epithelial BM components: The percentage formation of the individual BM components was quantitated using Adobe Photoshop CS5 version 12.0 (San Jose, CA). Using the ruler tool, individual images of the 3D cultures at 200× magnification were used for measuring the length of each BM component formed. The percentage formation was computed using the length of individual BM components assembled divided by the total length, then multiplied by 100. Images from six different batches of 3D organotypic cultures were analyzed to compute the mean ± SEM values. Statistical analyses were performed using GraphPad Prism version 9.0 (Boston, MA). The differences between the groups for individual BM components were compared using one-way ANOVA with Tukey's post-hoc test, and $p < 0.05$ was considered statistically significant.

Transmission electron microscopy: Transmission electron microscopy (TEM) samples were prepared using the method described by Fantes et al. [41]. Briefly, the 3D organotypic cultures were fixed by incubating in a 0.2-M cacodylate buffer containing 2.5% glutaraldehyde and 4% paraformaldehyde for 24 h. The specimens were then rinsed with a 0.2-M cacodylate buffer three times for 5 min each time. Then, they were post-fixed in 1% osmium tetroxide for 60 min at 4 °C. The samples were then dehydrated in increasing concentrations of ethanol from 30% to 95% for 5 min each at 4°C. Finally, dehydration was performed using three 10-min rinses in 100% ethanol and three 15-min rinses with propylene oxide at room temperature. Excised blocks of the specimens were then embedded in epoxy resin media, and 1-µm sections were prepared. The sections were stained with toluidine blue for orientation and light microscopy. Ultrathin 85-nm sections were prepared using a diamond knife stained with 5% uranyl acetate and lead citrate and observed using a Philips CM12 transmission electron microscope operated at 60 kV (FEI Company, Hillsboro, OR).

RESULTS

Light microscopy and ICC confirmation of cell morphology and phenotype: Light microscopic observations confirmed the morphology of the primary cultures used in this study. Fibroblasts showed long, elongated, and spindle structures; myofibroblasts showed a much larger contractile fusiform morphology; and corneal epithelial cells were found to have a more polygonal rounded morphology (Figure 1A). To confirm that the myofibroblasts used in this study were

fully differentiated, the cells were stained for myofibroblast markers. The cells derived from both sources—cornea (C Myo) and bone marrow (B Myo)—expressed vimentin, alpha-SMA, desmin, and vinculin, which confirmed the fully differentiated myofibroblast phenotype (Figure 1B). Non-specific isotypic antibodies were used as controls for each antibody tested (Figure 1B).

Corneal fibroblasts and corneal epithelial cells coordinate in epithelial BM assembly: The comparison between 3D cultures of corneal fibroblasts with epithelial cells (CFib + Epi), corneal myofibroblasts with epithelial cells (CMyo + Epi), and epithelial cells cultured alone (Epi only controls) for epithelial BM markers laminin alpha-5, perlecan, and nidogen-1 are shown in Figure 3A. The percentage assembly of the individual BM components are represented in Figure 3B. CFib + Epi expressed all three epithelial BM markers—laminin alpha-5, perlecan, and nidogen-1—as a thin layer at the interface between the epithelial cells and fibroblasts. This was suggestive of a well-assembled epithelial BM in 3D cultures of fibroblasts in combination with the epithelial cells, similar to that observed in the cornea in situ. Around 90% of the epithelial-stromal interface was occupied by the BM components. On average, there was 93% of laminin alpha-5 layer completed, 96% of perlecan layer completed, and 92% of the nidogen-1 layer completed in the epithelial BMs analyzed. Conversely, CMyo + Epi showed no evidence of a well-assembled epithelial BM. When epithelial cells were cultured with myofibroblasts, there was a significant decrease ($p < 0.001$) in the percentage of BM formed, showing only 5% of laminin alpha-5 formation and 2% of nidogen-1 formation, although perlecan occupied 20% of the epithelial BM region. It is important to note that almost all the myofibroblasts in the stroma expressed perlecan. This indicates that even though the myofibroblasts were able to synthesize perlecan, they were not able to assemble perlecan into an epithelial BM. Epithelial cells, when cultured alone above the collagen matrix, showed 69% of laminin alpha-5 formation, 49% of perlecan formation, and no evidence of nidogen-1 formation.

Appendix 1 shows the triplex IHC for laminin alpha-5, perlecan, and nidogen-1 in single cell controls cultured in a collagen matrix. Fibroblasts had very high expression of perlecan and moderate expression of laminin alpha-5 and nidogen-1. Myofibroblasts expressed perlecan but not nidogen-1.

Figure 4A shows IHC for other epithelial BM markers, such as laminin beta-3 and collagen type IV, in the 3D culture of CFib + Epi and CMyo + Epi. The percentage assembly of laminin beta-3 and collagen IV is shown in Figure 4B. Epithelial cells when cultured with fibroblasts showed evidence of a well-assembled epithelial BM, which was confirmed by the expression of laminin beta-3 and collagen IV at the interface between the fibroblasts and epithelial cells as well as in epithelial cells extending two to three layers above the epithelial BM. Furthermore, 97% of the epithelial BM region was occupied by laminin beta-3 and collagen IV. The formation of epithelial BM components decreased significantly ($p < 0.0001$) when epithelial cells were cultured alone or with myofibroblasts. There was only 2.3% of laminin beta-3 formation and 8.6% of collagen type IV formation in epithelial cells with myofibroblast 3D cultures. Though the myofibroblasts showed very high expression of collagen type IV in the stroma, it was not assembled onto the epithelial BM. Epithelial cells when cultured alone showed 67% of laminin beta-3 formation and 30% of collagen type IV formation. The respective stromal single cell controls for laminin beta-3 and collagen type IV expression are shown in Appendix 2. Both the fibroblasts and myofibroblasts when cultured alone expressed collagen type IV. Overall, this suggests that the laminin chains—laminin alpha-5 and laminin beta-3—of the BM were predominantly expressed by epithelial cells, and the stromal cells mainly contributed to the expression of perlecan, nidogen-1, and collagen IV.

For further validation, 3D cultures were prepared from two additional lots of epithelial cells procured from two different companies—Cell Applications (labeled as Epi 2) and Cell Biologics (labeled as Epi 3; Appendix 3). The fibroblasts and myofibroblasts derived from the same batches of primary cells were used with both lots of epithelial cells for a better comparison. In both these batches of 3D cultures, the formation of epithelial BM was observed only when epithelial cells were cultured in the presence of fibroblasts embedded in collagen. However, there was a mild difference in nidogen-1 expression between the two lots of epithelial cells when cultured with fibroblasts. Epithelial cells procured from Cell Biologics when cultured with fibroblasts showed a spotted patchy expression of nidogen-1, whereas the epithelial cells from Cell Applications showed more of a continuous nidogen-1 expression throughout the 3D culture. In all three batches of Epi 3 with fibroblast cultures, a patchy expression of nidogen-1 was observed in some areas and a continuous expression of nidogen-1 in other areas of the 3D cultures. To highlight the difference between both the epithelial cells, the ones with the least expression of nidogen-1 is shown in the figure. Though nidogen-1 is expressed by and mainly results from the fibroblasts in a 3D culture, the reason for the difference in nidogen-1 expression between the 3D cultures prepared from both lots of epithelial cells remains unclear.

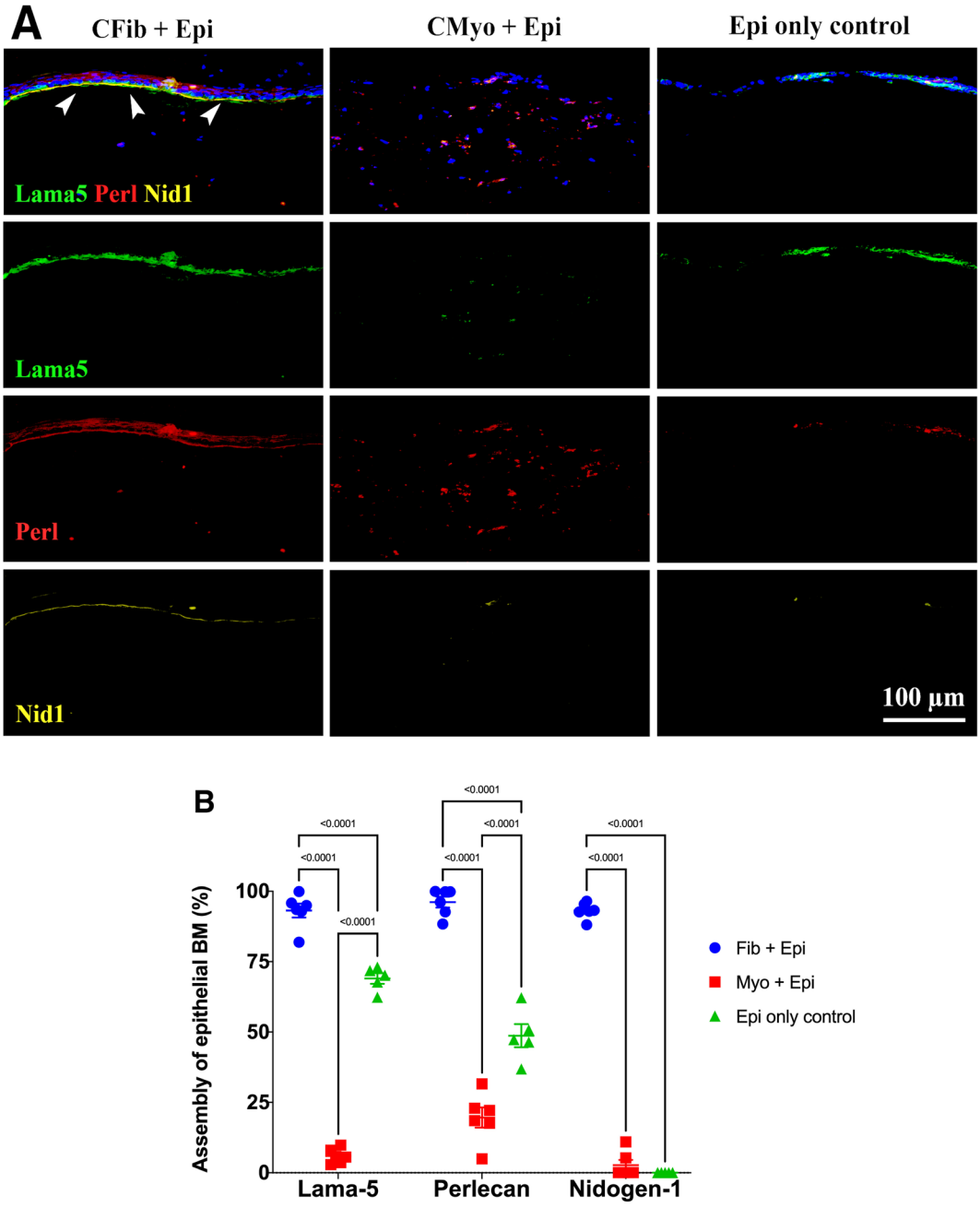

Figure 3. Comparison of laminin alpha 5, perlecan and nidogen-1 expression in different 3D cultures. **A**: Triplex immunohistochemistry (IHC) for laminin alpha-5, perlecan, and nidogen-1 in 3D corneal organotypic cultures. The corneal fibroblast and epithelial (CFib + Epi) organotypic cultures showed expression of laminin alpha-5 (green), perlecan (red), and nidogen-1 (yellow) at the interface between the epithelial cells and the fibroblasts, suggesting a well-assembled epithelial BM. In corneal myofibroblast and epithelium (CMyo + Epi) cultures, there was a high expression of perlecan, a lower expression of laminin alpha-5, and no expression of nidogen-1 detected. It is important to note that the expression was observed only in the stroma, and the overlying epithelial BM was not assembled when myofibroblasts were co-cultured with epithelial cells. When the epithelial cells were cultured alone above the collagen matrix (Epi only control), laminin alpha-5 was predominantly expressed throughout the epithelium, perlecan expression was low, and no expression of nidogen-1 was detected. Blue is DAPI staining of cell nuclei. Mag.: 200×. **B**: A graph showing the percentage assembly of individual epithelial BM components, comparing between the groups of 3D cultures. Error bars represent mean ± SEM. Each BM component was compared between the groups using one-way ANOVA, and $p < 0.05$ was considered statistically significantly different.

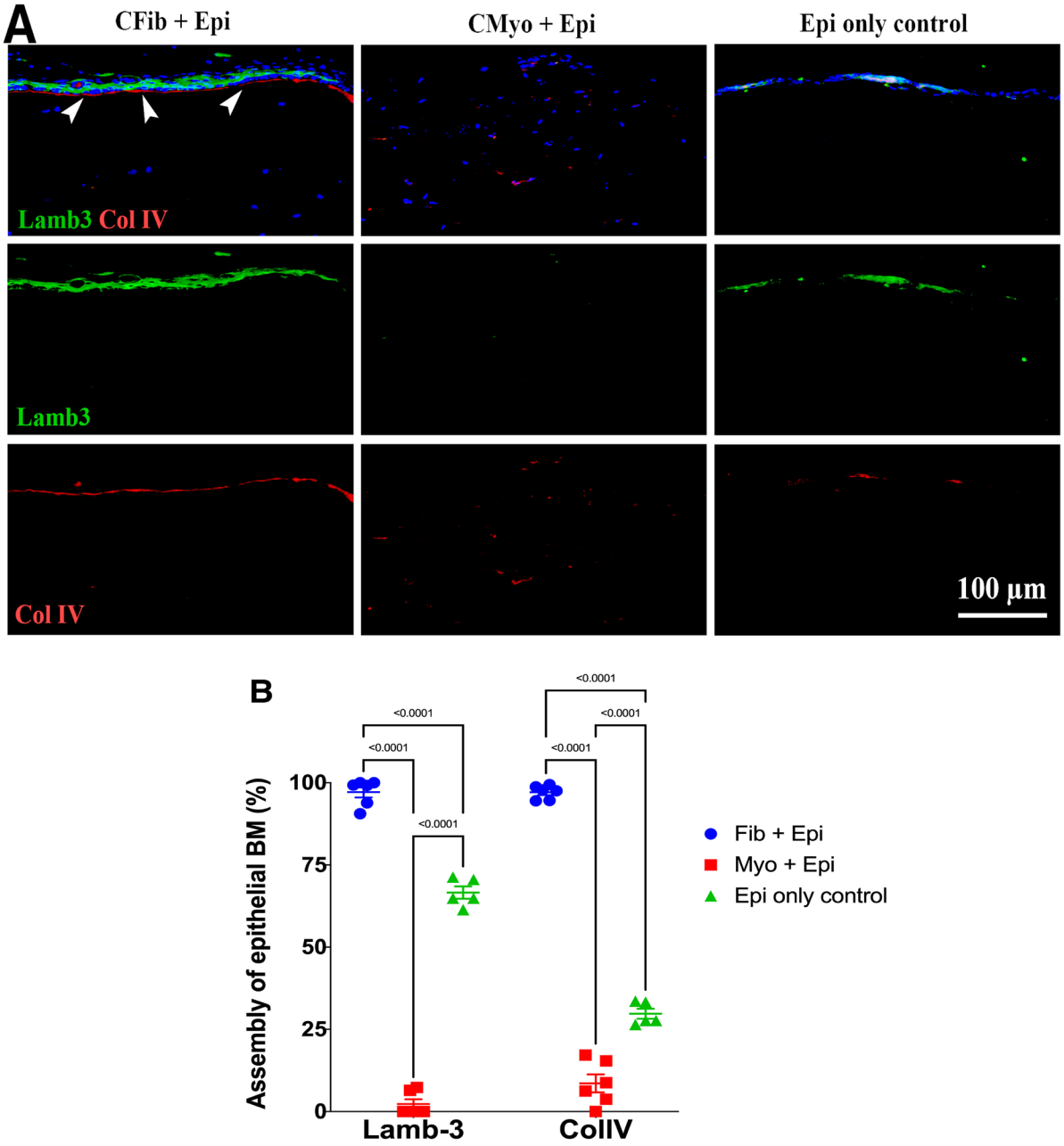

Figure 4. Comparison of laminin beta 3 and collagen IV expression in different 3D cultures. **A**: Duplex IHC for laminin beta-3 and collagen type IV in corneal organotypic cultures. The CFib + Epi cultures showed high expression of laminin beta-3 (green) in basal and more superficial epithelial layers. Collagen type IV (red) at the interface of the epithelial cells and fibroblasts indicates a normally regenerated epithelial BM. However, CMyo + Epi cells in organotypic cultures showed no evidence for epithelial BM generation, although myofibroblasts were found to produce collagen type IV. In Epi only controls, laminin beta-3 is expressed throughout the epithelium, with low expression of collagen type IV. Blue is DAPI staining of cell nuclei. Mag.: 200×. **B**: Graph showing percentage formation of laminin beta-3 and collagen IV compared between the groups of 3D cultures. Error bars represent mean ± SEM. One-way ANOVA was used to compare between the groups, and $p < 0.05$ was considered statistically significantly different.

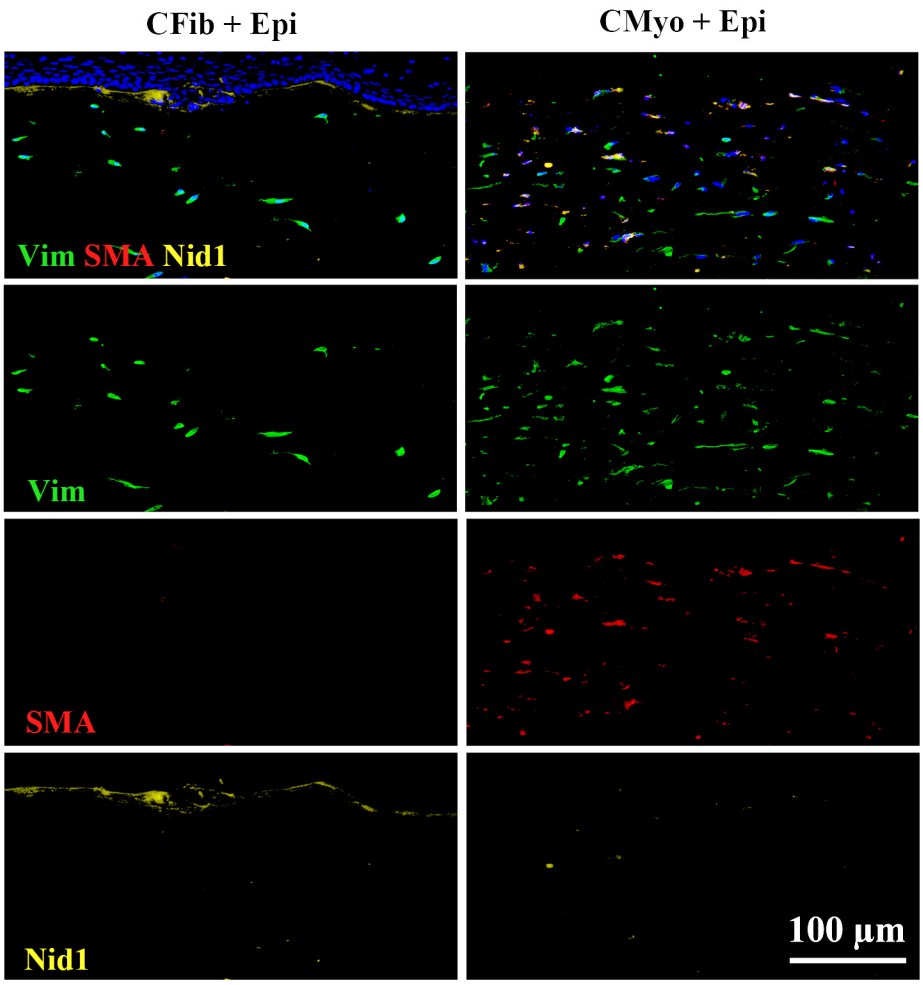

Figure 5. Triplex IHC for vimentin, alpha-SMA, and nidogen-1 in corneal organotypic cultures. Expression of vimentin (green), but no expression of alpha-SMA (red), indicates that the corneal fibroblasts retained their phenotype in CFib + Epi organotypic cultures even after 18 days of culture. Vimentin-positive corneal fibroblasts populated the matrix beneath the epithelium. Meanwhile, CMyo + Epi expressed both vimentin and alpha-SMA, indicative of the myofibroblast phenotype. Blue is DAPI staining of cell nuclei. Mag.: 200×.

Stromal cells maintained their phenotype in 3D organotypic culture: To confirm whether the stromal cells maintained their phenotype even at the end of 18 days of incubation in 3D cultures, they were stained for mesenchymal marker vimentin, myofibroblast marker alpha-SMA, and epithelial BM marker nidogen-1. CFib + Epi 3D cultures were found to express vimentin and not alpha-SMA. This confirmed that the corneal fibroblasts were not differentiated further in the 3D cultures, and the phenotype was well-maintained. CMyo + Epi had expression of both vimentin and alpha-SMA, confirming the myofibroblastic phenotype (Figure 5).

Myofibroblasts derived from both cornea and bone marrow could not assemble epithelial BM: During corneal wound healing after injury, the stroma is occupied by myofibroblasts derived from both corneal fibroblasts and bone marrow-derived fibrocytes [16]. To determine if combinations of these myofibroblasts were more effective in assembling epithelial BM, different 3D cultures were prepared with rabbit corneal epithelial cells in combination with 100% corneal myofibroblasts, 100% bone marrow-derived myofibroblasts, or a combination of 50% corneal and 50% bone marrow-derived myofibroblasts. Triplex IHC for laminin alpha-5, perlecan, and nidogen-1 revealed no evidence for an assembled epithelial BM in any of these combinations of myofibroblasts with epithelial cells. It was also noted that the epithelial cells did not form a typical stratified morphology in these cultures but rather appeared as one or two layers, epithelial spheroid-like structures, or no epithelium in different runs of the cultures (Figure 6).

Epithelial BM assembly in TEM images: To confirm epithelial BM assembly, CFib + Epi 3D cultures were processed and observed with TEM. Figure 7A confirms a multi-layered stratified epithelium when cultured in the presence of corneal fibroblasts in the stroma. Figure 7B confirms that fibroblasts were embedded and dispersed in the collagen matrix. The presence of a well-assembled epithelial BM is indicated by the arrows directly beneath the epithelial cells (Figure 7C,D).

Corneal fibroblasts and epithelial BM formation in rabbit corneas after PRK: Triplex IHC for mesenchymal marker vimentin, myofibroblast marker alpha-SMA, and epithelial BM marker nidogen-1 in rabbit corneas at different timepoints after −3D PRK are shown in Figure 8A,B. At 1 week after PRK, there was patchy expression of nidogen-1 with an irregular arrangement of epithelial cells. There was also evidence for few vimentin-positive, SMA-negative corneal fibroblasts at 1 week after PRK. Fibrocytes that had migrated into the cornea by 1 week after PRK were also vimentin positive and could not be distinguished by this IHC analysis but would undergo similar TGF beta-driven differentiation to myofibroblasts. Thus, at least two myofibroblast precursor cells would be present if cell-specific IHC was performed [16]. At 2 weeks after PRK, an increase in the number of vimentin-positive, SMA-negative cells was observed in the

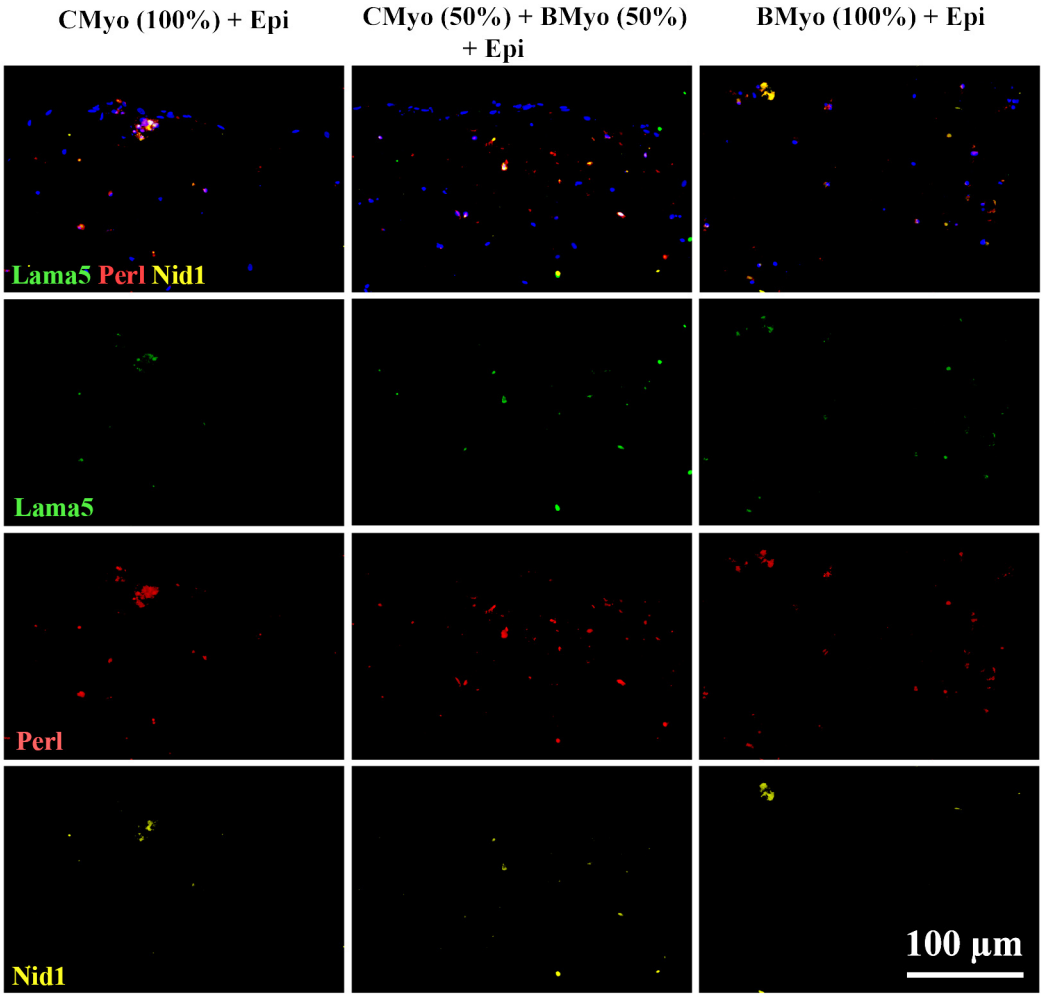

Figure 6. IHC for laminin alpha-5, perlecan, and nidogen-1 in CMyo + Epi organotypic cultures. Triplex IHC did not detect epithelial BM posterior to the epithelium in this example culture or any other corneal myofibroblast, bone marrow-derived myofibroblast, or mixed corneal-bone marrow myofibroblast organotypic culture with corneal epithelium. Also, no stratified epithelium was detected in these cultures. This indicates that the myofibroblasts derived from both cornea and bone marrow—either alone as CMyo (100%)/BMyo (100%) or combined (CMyo 50% + BMyo 50%)—when incubated with corneal epithelial cells could not assemble BM. Rather, spheroid-like epithelial masses were present in many cultures. Myofibroblasts were observed throughout the matrix. Blue is DAPI staining of the nuclei. Mag.: 200×.

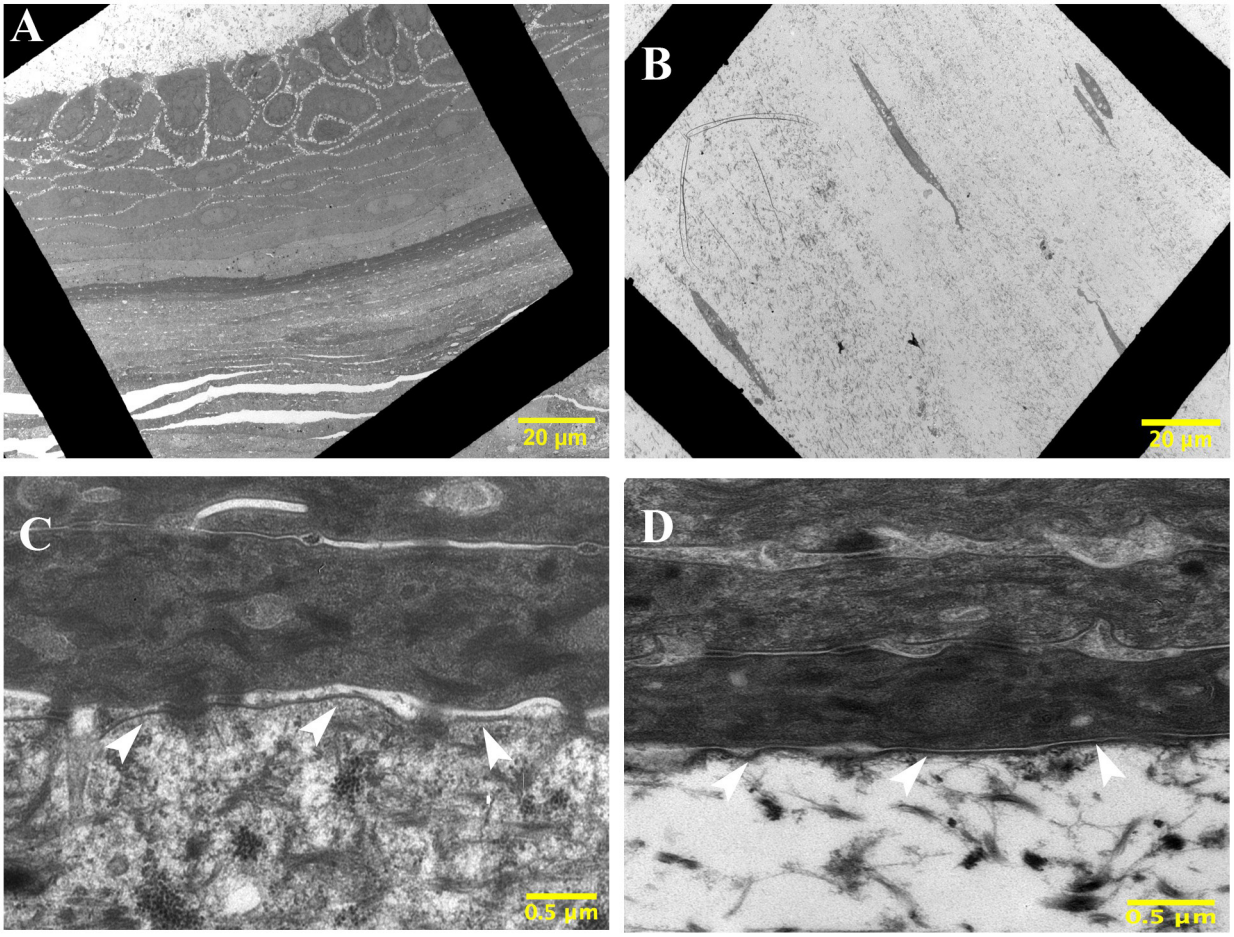

Figure 7. Transmission electron microscopy (TEM) showing epithelial BM assembly. **A**: The presence of a well-orchestrated, multi-layered stratified epithelium when cultured in the presence of fibroblasts in the stroma (Mag.: 890×). **B**: The presence of fibroblasts embedded and dispersed in the collagen matrix (Mag.: 890×). **C**,**D**: The presence of a well-assembled epithelial BM when co-cultured with corneal fibroblasts, as indicated by arrows directly beneath the epithelial cells (Mag.: 30,000×).

anterior stroma, with epithelial BM still observed only in patches (Figure 8A).

At 4 weeks after PRK, there was a notable increase in the number of vimentin-positive, SMA-negative cells in the anterior stroma, with an 80–90% regenerated epithelial BM. This suggests a strong association with CFib + Epi BM reassembly at 4 weeks after PRK surgery. At 6 weeks after PRK, the percentage of regenerated epithelial BM was further increased, and the number of corneal fibroblasts and/or fibrocytes in the subepithelial stroma was decreased. At 8 weeks after PRK, the epithelial BM was fully regenerated, and the vimentin-positive, SMA-negative cells had disappeared from the subepithelial stroma (Figure 8B). Since the rabbit corneas were treated with low correction −3D PRK, there was no fibrosis observed in these corneas and hence no alpha-SMA-positive myofibroblasts in the subepithelial stroma [17]. This demonstrates that in a corneal injury model, there is formation of an active repair corneal fibroblast phenotype at the site of injury, and these cells likely play an active role in epithelial BM regeneration.

DISCUSSION

The results of this study confirm that corneal epithelial cells and corneal fibroblasts cooperate to produce epithelial BM in organotypic cultures detected with electron microscopy and IHC for epithelial BM markers laminin alpha-5, laminin beta-3, perlecan, nidogen-1, and collagen type IV. Conversely, cornea-derived myofibroblasts, bone marrow-derived myofibroblasts, and a combination of these myofibroblasts did not generate epithelial BM when in organotypic cultures with corneal epithelial cells. Further evidence was provided in a rabbit corneal wound healing model in situ. In rabbits treated with −3D PRK, the anterior stroma was predominantly

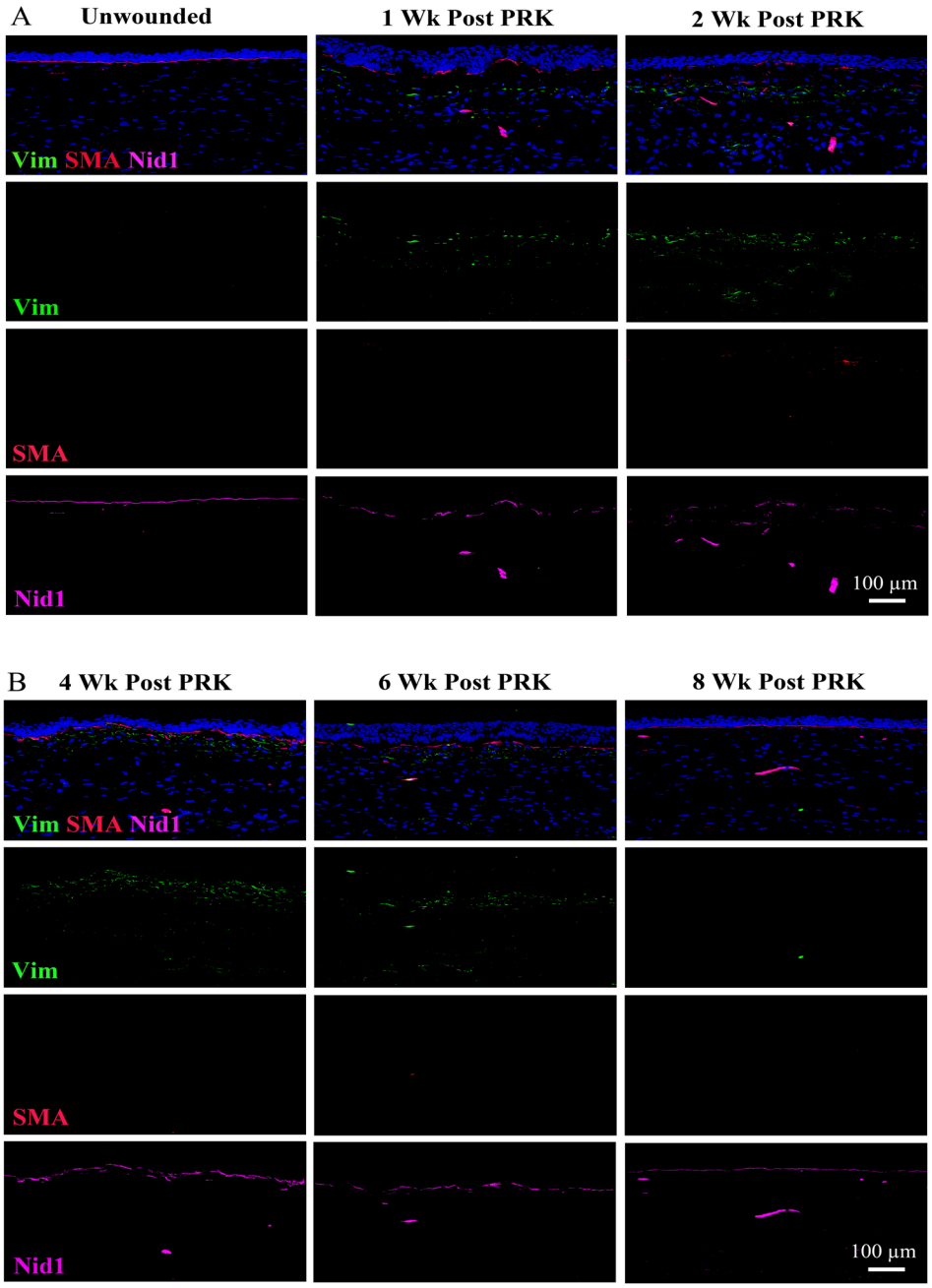

Figure 8. Comparison of rabbit corneas at different time points after Photorefractive Keratectomy surgeries. **A**, **B**: Triplex IHC for vimentin, SMA, and nidogen-1 in corneas at different time points after PRK surgeries. Triplex IHC for mesenchymal marker vimentin (green), myofibroblast marker alpha-SMA (red), and epithelial BM marker nidogen-1 (magenta) was observed in rabbit corneas at different time points after −3D PRK. At 1 and 2 weeks after PRK, there was a patchy expression of nidogen-1 with irregular cellular arrangement of epithelial cells. There was evidence for few vimentin-positive fibroblasts at both of these time points, and vimentin-positive fibrocytes could also be present in the anterior stroma. At 4 weeks after PRK, there was an increase in the number of vimentin-positive cells in the anterior stroma. In parallel, there was an increase in the percentage of epithelial BM regenerated to around 80–90%. This suggests a strong association of fibroblasts with epithelial BM regeneration at 4 weeks after PRK injury. At 6 weeks after PRK, when the percentage of epithelial BM regeneration was further increased, the corneal fibroblast numbers had decreased. At 8 weeks after PRK, most vimentin-positive cells disappeared from the anterior stroma, when the epithelial BM was fully regenerated. No alpha-SMA-positive cells were observed at any of the time points tested, indicating there was no fibrosis in these corneas. Blue is DAPI staining of the nuclei. Mag.: 200×.

occupied by corneal fibroblast cells, although fibrocytes were also likely present in the subepithelial stroma [16,25]. The strong association between the fibroblasts and BM regeneration further supports the important role of corneal fibroblasts in epithelial BM reassembly after injury.

Prior studies have reported the contribution of fibroblasts in the regeneration of the epithelial BM in other organotypic cultures and tissue engineered models such as the skin, lungs, breasts, gut, and kidneys [29-34]. In a human skin equivalent model, reconstruction of the BM was regulated by fibroblasts and/or exogenous activated keratinocytes [42]. This was confirmed in two different matrix systems—collagen and de-epidermized dermis. In tissue-engineered skin, superficial dermal fibroblasts were found to enhance BM formation and barrier function of the epithelium [34,43]. MLE-15 respiratory epithelial cells grown on fibroblast-embedded collagen gels also assembled BM-like structures with expression of laminin alpha-5 [44]. On fibroblast-embedded collagen gels, SV40-T2 transfected alveolar epithelial cells formed a continuous thin layer of BM, whereas on collagen gels without fibroblasts, SV40-T2 cells produced only discontinuous diffuse deposits [30].

When epithelial cells were cultured alone or in combination with myofibroblasts, only one or two layers of epithelium typically formed, and in some instances, no epithelial layer was present. Only when the epithelial cells were cultured with corneal fibroblasts embedded in the collagen did they form a multi-layered stratified epithelium [5]. Laminin beta-3 expression was unique to epithelial cells, and nidogen-1 expression was unique to corneal fibroblasts. Although laminin beta-3 is produced only by epithelial cells, a previous study reported that the presence of fibroblasts was important for integrating laminin beta-3 into BM in skin co-cultures [45]. Apart from the epithelial BM components, there might be other microenvironmental factors released from fibroblasts that contribute to epithelial functions such as adhesion, growth, and proliferation [46]. Diffusible factors produced by fibroblasts could modulate the keratinocyte production of BM components in skin [47], and this stromal-epithelial regulation could also be present in the cornea. Only tissues and 3D cultures with well-assembled BMs showed optimal epithelial tissue architecture.

The formation of the BM could also coordinate epithelial cell polarity [48]. For example, in lung organotypic cultures, blocking laminin polymerization inhibited the formation of polarized epithelial cysts [49,50].

Previous studies reported mRNA and protein expression of epithelial BM components, such as laminin, perlecan, and nidogen, by corneal stromal cells (corneal fibroblasts and myofibroblasts). In an in vitro study, keratocytes had nidogen-2 and perlecan proteins predominantly in intracellular compartments, whereas in myofibroblasts, these epithelial BM components were observed diffusely throughout the cell and were not capable of localizing the epithelial BM components to the nascent BM [51]. Thus, the lack of epithelial BM generation when corneal epithelial cells are in an organotypic culture with myofibroblasts was likely attributable to myofibroblasts lacking the capacity to coordinate with epithelial cells in the insertion of BM components into the nascent epithelial BM.

Corneal epithelial cells did not form a typical stratified morphology when co-cultured with corneal or bone marrow-derived myofibroblasts. Though the exact reasons remain unknown, this could be attributed to epithelial mesenchymal transition (EMT) induced by TGF β-1, contraction of collagen, and remodeling of the ECM induced by myofibroblasts. EMT has been reported as a prominent effect of TGF beta-1 in various tissues and co-culture models [52,53]. In a human bronchial co-culture of mesenchymal cells with epithelial cells, TGF beta-1 treatment showed a concentration-dependent decrease in the thickness of the epithelial cell layer [54]. This was confirmed through a significant increase in the number of vimentin-positive and alpha SMA-positive mesenchymal cells with a significant decrease in the expression of epithelial junction molecule E-cadherin in the epithelial cell layer when treated with 10 ng/ml of TGF beta-1 for 21 days. This clearly indicated that TGF beta-1 treatment induced transition of epithelial cells into mesenchymal cells in the epithelial cell layer of the 3D co-culture system [54]. Similarly, the correlation between TGF beta-1 and EMT was also demonstrated in a lung epithelial–macrophage co-culture model [54]. The elevated levels of TGF beta-1 in the media secreted by macrophages stimulated the transition of epithelial cells into mesenchymal cells [55]. Further, lung epithelial cells co-cultured with myofibroblasts lost their ability to form organoids in vitro, whereas fibroblasts supported organoid formation. This is partially attributed to the Wnt/beta catenin pathway skewing as a result of TGF beta-1-induced myofibroblast differentiation [56].

In a human bronchial tissue 3D co-culture model of epithelial cells with mesenchymal cells, TGF beta-1 exerted a concentration-dependent effect on collagen contraction and induced structural changes in 3D cultures. TGF beta-1 treatment at 10 ng/ml for 21 days showed a significant increase in collagen gel contraction compared to untreated controls [54]. Apart from 3D cultures, the enhanced collagen contraction effect of TGF beta-1 was observed even in submerged cultures [57,58]. Cardiac fibroblasts treated with TGF beta-1 showed an enhanced collagen contractile activity through

differentiation of myofibroblasts. The increase in the collagen contractile activity was directly proportional to the increase in myofibroblast formation [59]. In trabecular meshwork cells, TGF beta-1 induced collagen contraction through the activation of Rho and Ca^{2+}-dependent enzymes protein kinase C and myosin light chain kinase [60]. Further, the enhanced collagen contraction effect of TGF beta-1 was also observed in different tissue fibroblasts such as the placenta [61], skin [62], buccal mucosa [63], heart [64], and kidneys [65].

In contrast, intestinal epithelial cell line Caco2 co-cultured with mesenchymal cells for 14 days was shown to produce a BM-like structure with expression of laminin, collagen IV, fibronectin, and heparan sulfate proteoglycans [66]. This epithelial–myofibroblasts co-culture system was later used to study intestinal epithelial wound healing [67].

In rabbit corneas treated with a low-correction non-fibrotic −3.0D PRK, the regeneration of epithelial BM showed a strong association with the formation of an active repair corneal fibroblast phenotype in the sub-epithelial stroma. Because the corneas were treated only with a low-correction PRK, no fibrosis was expected, and so there was no formation of alpha-SMA-positive myofibroblasts at the site of injury. The sub-epithelial and the anterior stroma were mostly populated with vimentin-positive fibroblasts. At early time points post-PRK, the vimentin-positive cells could also be fibrocytes derived from bone marrow [17,27]. In the initial few weeks after PRK, defective epithelial BM regeneration, which altered the epithelial stromal interaction, was observed [68]. This also allowed for the diffusion of growth factors such as fibroblast growth factor (FGF) and cytokines in the stroma, which trigger the formation of fibroblasts. At 4 weeks after PRK, 80–90% of the epithelial BM was regenerated, as indicated by the nidogen-1 expression. Meanwhile, the anterior stroma was also populated with vimentin-positive alpha-SMA-negative fibroblasts at this time point. Nidogen-1 and perlecan act as bridging molecules inter-connecting the laminin and collagen IV networks, thus maintaining the stability and structure of epithelial BM [69]. Based on previous in vitro laboratory findings and rabbits treated with non-fibrotic −4.5D PRK, it is known that the stromal cells primarily contributed perlecan, nidogen-1, and collagen IV expression, although epithelial cells mainly produced laminin alpha-5 and laminin beta-3 in a regenerating epithelial BM [68,70].

The regeneration of BM acts as a barrier to tear- and epithelium-derived pro-fibrotic growth factors [11]. This also inhibits the production of growth factors by the corneal epithelial cells. This is likely the reason why at the end of 8 weeks after PRK, the formation of a fully-regenerated epithelial BM showed no evidence of vimentin-positive fibroblasts in the stroma. The regeneration of epithelial BM also regulates the movement of growth factors, such as HGF and KGF, from the stroma to the epithelium [18,20]. The reduced availability of growth factors limits epithelial hyperplasia and hypertrophy, which are commonly observed at earlier time points, and returns the epithelium to its normal morphology once the epithelial BM is fully regenerated. Prior studies have also confirmed that at 8 weeks after −4.5D PRK, the stroma is populated only with keratocytes [68]. Because of the lack of availability of growth factors, it is likely that the fibroblasts either dedifferentiated into keratocytes or underwent apoptosis. This study confirmed that even in cornea with mild injuries (when there is no formation of myofibroblasts), there is formation of fibroblasts, which in coordination with epithelial cells regenerate the epithelial BM.

Approximately 2 weeks of organotypic cultures appeared to be optimal for corneal epithelial cells and corneal fibroblasts to generate epithelial BM with normal morphology, which was analyzed using IHC for BM components. Thus, these organotypic cultures appear to be an optimal model for studying the interactions between corneal epithelial and fibroblast cells involved in epithelial BM regeneration and possibly in experiments to explore the role of the epithelial BM in modulating the localization—and therefore function—of tear and epithelium-derived growth factors (e.g., TGF beta-1) and corneal fibroblast-derived growth factors (e.g., HGF and KGF/FGF-7) [18]. These organotypic cultures should also be useful for studying the effects of other epithelial and stromal cytokines (e.g., interleukin-1 alpha) and growth factors (e.g., PDGF) on epithelial BM regeneration [12,21].

The major limitation of this study is that the 3D organotypic cultures were established only for a single time point. Having multiple time points to observe the progress of the 3D culture might facilitate study of the exact time point at which the epithelial BM started to assemble. It may also help reveal which components are responsible for early epithelial BM development, although the literature strongly supports the role of epithelial cell-produced laminins, such as laminin alpha-5, in beginning the formation of the epithelial BM [4,50]. The authors increased the incubation time to 30 days in some experiments to determine if a longer incubation resulted in the formation of epithelial BM in co-cultures with myofibroblasts. However, myofibroblasts and epithelial cells did not produce epithelial BM even with the longer culture time.

It remains to be determined precisely how the BM components released by fibroblasts and epithelial cells are targeted at the stromal–epithelial interface and are correctly

organized and integrated within the matrix. In future studies, the mode of communication between the fibroblast and epithelial cells in assembling the BM needs to be further elucidated.

APPENDIX 1. SINGLE CELL CONTROLS SHOWING EXPRESSION FOR LAMININ ALPHA 5, PERLECAN AND NIDOGEN-1.

To access the data, click or select the words "Appendix 1." Representative IHC for laminin alpha-5, perlecan, and nidogen-1 in organotypic cultures prepared with a single cell type. Corneal fibroblasts when cultured alone, showed expression of perlecan and nidogen-1, but very low laminin alpha-5 expression. In corneal myofibroblasts, the expression of laminin alpha-5 and perlecan is less compared to the corneal fibroblasts, with very low to no expression of nidogen-1 in each batch cultured. Blue is DAPI stained nuclei. Mag. 200X.

APPENDIX 2. SINGLE CELL CONTROLS SHOWING EXPRESSION FOR LAMININ BETA 3 AND COLLAGEN IV.

To access the data, click or select the words "Appendix 2." Representative IHC for laminin beta-3 and perlecan in organotypic cultures prepared with a single cell type. Both corneal fibroblasts and myofibroblasts expressed collagen type IV, but no expression of laminin beta-3, when cultured alone. Blue is DAPI stained nuclei. Mag. 200X.

APPENDIX 3. COMPARISON OF 3D CULTURES PREPARED FROM TWO DIFFERENT BATCH OF EPITHELIAL CELLS.

To access the data, click or select the words "Appendix 3." Triplex IHC for laminin alpha-5, perlecan and nidogen-1 in 3D cultures prepared with two different batches of epithelial cells. Epithelial cells procured commercially from two different companies—Cell Applications (labeled as Epi2) and Cell Biologics (labeled as Epi 3)—were used to prepare 3D cultures in combination with corneal fibroblasts or myofibroblasts generated from corneal fibroblasts. The fibroblasts and myofibroblasts derived from the same batches of primary cells were used with both lots of epithelial cells for better comparison. The formation of a well assembled epithelial BM, observed via the presence of laminin alpha-5 (green), perlecan (red) and nidogen-1 (yellow) as a thin sheet, only when epithelial cells are cultured in the presence of corneal fibroblasts in the collagen matrix. No evidence for epithelial BM assembly was observed when the epithelial cells are cultured with myofibroblasts. Blue is DAPI stained nuclei. Mag. 200X.

ACKNOWLEDGMENTS

We gratefully acknowledge Peter Yurchenco, PhD, New Brunswick, NJ for providing laminin alpha-5 antibody, and Mei Yin, Imaging Core, Cleveland Clinic, for the support in performing transmission electron microscopy. Funding Supported by the Department of Defense grants VR210001 (SEW) and VR180066 (SEW), US Public Health Service grant EY025585 from NEI, Research to Prevent Blindness, New York, NY, and and The Cleveland Eye Bank Foundation, Cleveland, OH.

REFERENCES

1. Thesleff I, Vaahtokari A, Partanen AM. Regulation of organogenesis. Common molecular mechanisms regulating the development of teeth and other organs. Int J Dev Biol 1995; 39:35-50. [PMID: 7626420].
2. Parmar H, Cunha GR. Epithelial-stromal interactions in the mouse and human mammary gland in vivo. Endocr Relat Cancer 2004; 11:437-58. [PMID: 15369447].
3. Strand DW, Hayward SW. Modelling stromal-epithelial interactions in disease progression. Discov Med 2010; 9:504-11. [PMID: 20587339].
4. Pozzi A, Yurchenco PD, Iozzo RV. The nature and biology of basement membranes. Matrix Biol 2017; 57-58:1-11. [PMID: 28040522].
5. El Ghalbzouri A, Lamme E, Ponec M. Crucial role of fibroblasts in regulating epidermal morphogenesis. Cell Tissue Res 2002; 310:189-99. [PMID: 12397374].
6. Halfter W, Oertle P, Monnier CA, Camenzind L, Reyes-Lua M, Hu H, Candiello J, Labilloy A, Balasubramani M, Henrich PB, Plodinec M. New concepts in basement membrane biology. FEBS J 2015; 282:4466-79. [PMID: 26299746].
7. Xing Q, Parvizi M, Lopera-Higuita M, Griffiths LG. Basement membrane proteins modulate cell migration on bovine pericardium extracellular matrix scaffold. Sci Rep 2021; 11:4607-[PMID: 33633241].
8. Khalilgharibi N, Mao Y. To form and function: on the role of basement membrane mechanics in tissue development, homeostasis and disease. Open Biol 2021; 11:200360-[PMID: 33593159].
9. Yurchenco PD, Ruben GC. Basement membrane structure in situ: evidence for lateral associations in the type IV collagen network. J Cell Biol 1987; 105:2559-68. [PMID: 3693393].
10. Jayadev R, Sherwood DR. Basement membranes. Curr Biol 2017; 27:R207-11. [PMID: 28324731].
11. Wilson SE, Torricelli AAM, Marino GK. Corneal epithelial basement membrane: Structure, function and regeneration. Exp Eye Res 2020; 194:108002-[PMID: 32179076].

12. Jester JV, Huang J, Petroll WM, Cavanagh HD. TGF beta induced myofibroblast differentiation of rabbit keratocytes requires synergistic TGF beta, PDGF and integrin signalling. Exp Eye Res 2002; 75:645-57. [PMID: 12470966].

13. Huh MI, Chang Y, Jung JC. Temporal and spatial distribution of TGF-beta isoforms and signalling intermediates in corneal regenerative wound repair. Histol Histopathol 2009; a24:1405-16. [PMID: 19760590].

14. Huh MI, Kim YH, Park JH, Bae SW, Kim MH, Chang Y, Kim SJ, Lee SR, Lee YS, Jin EJ, Sonn JK, Kang SS, Jung JC. Distribution of TGF-beta isoforms and signalling intermediates in corneal fibrotic wound repair. J Cell Biochem 2009; b108:476-88. [PMID: 19626665].

15. Singh V, Santhiago MR, Barbosa FL, Agrawal V, Ambati BK, Singh N, Wilson SE. Effect of TGFβ and PDGF-B blockade on corneal myofibroblast development in mice. Exp Eye Res 2011; 93:810-7. [PMID: 21978952].

16. Lassance L, Marino GK, Medeiros CS, Thangavadivel S, Wilson SE. Fibrocyte migration, differentiation and apoptosis during the corneal wound healing response to injury. Exp Eye Res 2018; 170:177-87. [PMID: 29481786].

17. de Oliveira RC, Tye G, Sampaio LP, Shiju TM, Dedreu J, Menko S, Santhiago MR, Wilson SE. TGF beta1 and TGF beta2 proteins in corneas with and without stromal fibrosis: Delayed regeneration of epithelial barrier function and the epithelial basement membrane in corneas with stromal fibrosis. Exp Eye Res 2021; 202:108325-[PMID: 33263285].

18. Wilson SE, Walker JW, Chwang EL, He YG. Hepatocyte growth factor, keratinocyte growth factor, their receptors, fibroblast growth factor receptor-2, and the cells of the cornea. Invest Ophthalmol Vis Sci 1993; 34:2544-61. [PMID: 8392040].

19. Tervo T, Vesaluoma M, Bennett GL, Schwall R, Helena M, Liang Q, Wilson SE. Tear hepatocyte growth factor (HGF) availability increases markedly after excimer laser surface ablation. Exp Eye Res 1997; 64:501-14. [PMID: 9227267].

20. Liang Q, Mohan RR, Chen L, Wilson SE. Signaling by HGF and KGF in corneal epithelial cells: Ras/MAP kinase and Jak-STAT pathways. Invest Ophthalmol Vis Sci 1998; 39:1329-38. [PMID: 9660480].

21. Kim WJ, Mohan RR, Mohan RR, Wilson SE. Effect of PDGF, IL-1alpha, and BMP2/4 on corneal fibroblast chemotaxis: expression of the platelet-derived growth factor system in the cornea. Invest Ophthalmol Vis Sci 1999; 40:1364-72. [PMID: 10359318].

22. Wilson SE, Liang Q, Kim WJ. Lacrimal gland HGF, KGF and EGF mRNA levels increase after corneal epithelial wounding. Invest Ophthalmol Vis Sci 1999; 40:2185-90. [PMID: 10476782].

23. West-Mays JA, Dwivedi DJ. The keratocyte: corneal stromal cell with variable repair phenotypes. Int J Biochem Cell Biol 2006; 38:1625-31. [PMID: 16675284].

24. Maruri DP, Miron-Mendoza M, Kivanany PB, Hack JM, Schmidtke DW, Petroll WM, Varner VD. ECM Stiffness Controls the Activation and Contractility of Corneal Keratocytes in Response to TGF-β1. Biophys J 2020; 119:1865-77. [PMID: 33080219].

25. Wilson SE, Sampaio LP, Shiju TM, Hilgert GSL, de Oliveira RC. Corneal opacity: Cell biological determinants of the transition from transparency to transient haze to scarring fibrosis, and resolution, after injury. Invest Ophthalmol Vis Sci 2022; 63:22-[PMID: 35044454].

26. Mohan RR, Kempuraj D, D'Souza S, Ghosh A. Corneal stromal repair and regeneration. Prog Retin Eye Res 2022; 91:101090-[PMID: 35649962].

27. Wilson SE, Sampaio LP, Shiju TM, de Oliveira RC. Fibroblastic and bone marrow derived cellularity in the corneal stroma. Exp Eye Res 2021; 202:108303-[PMID: 33068626].

28. Guo X, Hutcheon AEK, Zieske JD. Molecular insights on the effect of TGFb1/b3 in human corneal fibroblasts. Exp Eye Res 2016; 146:233-41. [PMID: 26992778].

29. Simon-Assmann P, Bouziges F, Arnold C, Haffen K, Kedinger M. Epithelial-mesenchymal interactions in the production of basement membrane components in the gut. Development 1988; 102:339-47. [PMID: 17061377].

30. Furuyama A, Kimata K, Mochitate K. Assembly of basement membrane in vitro by cooperation between alveolar epithelial cells and pulmonary fibroblasts. Cell Struct Funct 1997; 22:603-14. [PMID: 9591052].

31. Smola H, Stark HJ, Thiekötter G, Mirancea N, Krieg T, Fusenig NE. Dynamics of basement membrane formation by keratinocyte-fibroblast interactions in organotypic skin culture. Exp Cell Res 1998; 239:399-410. [PMID: 9521858].

32. Vidi PA, Bissell MJ, Lelièvre SA. Three-dimensional culture of human breast epithelial cells: the how and the why. Methods Mol Biol 2013; 945:193-219. [PMID: 23097109].

33. Tjin MS, Chua AWC, Moreno-Moral A, Chong LY, Tang PY, Harmston NP, Cai Z, Petretto E, Tan BK, Tryggvason K. Biologically relevant laminin as chemically defined and fully human platform for human epidermal keratinocyte culture. Nat Commun 2018; 9:4432-[PMID: 30377295].

34. Roger M, Fullard N, Costello L, Bradbury S, Markiewicz E, O'Reilly S, Darling N, Ritchie P, Määttä A, Karakesisoglou I, Nelson G, von Zglinicki T, Dicolandrea T, Isfort R, Bascom C, Przyborski S. Bioengineering the microanatomy of human skin. J Anat 2019; 234:438-55. [PMID: 30740672].

35. McKay TB, Guo X, Hutcheon AEK, Karamichos D, Ciolino JB. Methods for investigating corneal cell interactions and extracellular vesicles in vitro. Curr Protoc Cell Biol 2020; 89:e114-[PMID: 32986311].

36. Saikia P, Crabb JS, Dibbin LL, Juszczak MJ, Willard B, Geeng-Fu J, Shiju TM, Crabb JW, Wilson SE. Quantitative proteomic comparison of myofibroblasts derived from bone marrow and cornea. Sci Rep 2020; 10:16717-28. [PMID: 33028893].

37. Li L, Fukunga-Kalabis M, Herlyn M. The three-dimensional human skin reconstruct model: a tool to study normal skin

and melanoma progression. J Vis Exp 2011; 54:2937-[PMID: 21847077].

38. Shiju TM, Wilson SE. 3D in vitro corneal models: a review of current technologies. Exp Eye Res 2020; 200:108213-[PMID: 32890484].

39. Marino GK, Santhiago MR, Santhanam A, Torricelli AAM, Wilson SE. Regeneration of defective epithelial basement membrane and restoration of corneal transparency after photorefractive keratectomy. J Refract Surg 2017; 33:337-46. [PMID: 28486725].

40. Chaurasia SS, Kaur H, Medeiros FW, Smith SD, Wilson SE. Dynamics of the expression of intermediate filaments vimentin and desmin during myofibroblast differentiation after corneal injury. Exp Eye Res 2009; 89:133-9. [PMID: 19285070].

41. Fantes FE, Hanna KD, Waring GO, Pouliquen Y, Thompson KP, Savoldelli M. Wound healing after excimer laser keratomileusis (photorefractive keratectomy) in monkeys. Arch Ophthalmol 1990; 108:657-665. [PMID: 2334323].

42. El Ghalbzouri A, Jonkman MF, Dijkman R, Ponec M. Basement membrane reconstruction in human skin equivalents is regulated by fibroblasts and/or exogenously activated keratinocytes. J Invest Dermatol 2005; 124:79-86. [PMID: 15654956].

43. Varkey M, Ding J, Tredget EE. Superficial dermal fibroblasts enhance basement membrane and epidermal barrier formation in tissue-engineered skin: implications for treatment of skin basement membrane disorders. Tissue Eng Part A 2014; 20:540-52. [PMID: 24004160].

44. Nguyen NM, Bai Y, Mochitate K, Senior RM. Laminin alpha-chain expression and basement membrane formation by MLE-15 respiratory epithelial cells. Am J Physiol Lung Cell Mol Physiol 2002; 282:L1004-11. [PMID: 11943665].

45. Aumailley M. Laminins and interaction partners in the architecture of the basement membrane at the dermal-epidermal junction. Exp Dermatol 2021; 30:17-24. [PMID: 33205478].

46. Andriani F, Margulis A, Lin N, Griffey S, Garlick JA. Analysis of microenvironmental factors contributing to basement membrane assembly and normalized epidermal phenotype. J Invest Dermatol 2003; 120:923-31. [PMID: 12787116].

47. El Ghalbzouri A, Ponec M. Diffusible factors released by fibroblasts support epidermal morphogenesis and deposition of basement membrane components. Wound Repair Regen 2004; 12:359-67. [PMID: 15225215].

48. Tsutsui K, Machida H, Nakagawa A, Ahn K, Morita R, Sekiguchi K, Miner JH, Fujiwara H. Mapping the molecular and structural specialization of the skin basement membrane for inter-tissue interactions. Nat Commun 2021; 12:2577-[PMID: 33972551].

49. Klein G, Langegger M, Timpl R, Ekblom P. Role of laminin A chain in the development of epithelial cell polarity. Cell 1988; 55:331-41. [PMID: 3048705].

50. O'Brien LE, Jou TS, Pollack AL, Zhang Q, Hansen SH, Yurchenco P, Mostov KE. Rac1 orientates epithelial apical polarity through effects on basolateral laminin assembly. Nat Cell Biol 2001; 3:831-8. [PMID: 11533663].

51. Santhanam A, Torricelli AAM, Wu J, Marino GK, Wilson SE. Differential expression of epithelial basement membrane components nidogens and perlecan in corneal stromal cells in vitro. Mol Vis 2015; 21:1318-27. [PMID: 26788024].

52. Katsuno Y, Lamouille S, Derynck R. TGF-β signaling and epithelial-mesenchymal transition in cancer progression. Curr Opin Oncol 2013; 25:76-84. [PMID: 23197193].

53. Hackett TL, Warner SM, Stefanowicz D, Shaheen F, Pechkovsky DV, Murray LA, Argentieri R, Kicic A, Stick SM, Bai TR, Knight DA. Induction of epithelial-mesenchymal transition in primary airway epithelial cells from patients with asthma by transforming growth factor-beta1. Am J Respir Crit Care Med 2009; 180:122-33. [PMID: 19406982].

54. Ishikawa S, Ishimori K, Ito S. A 3D epithelial-mesenchymal co-culture model of human bronchial tissue recapitulates multiple features of airway tissue remodelling by TGF-β1 treatment. Respir Res 2017; 18:195-[PMID: 29166920].

55. Zhu L, Fu X, Chen X, Han X, Dong P. M2 macrophages induce EMT through the TGF-β/Smad2 signaling pathway. Cell Biol Int 2017; 41:960-8. [PMID: 28493530].

56. Ng-Blichfeldt JP, de Jong T, Kortekaas RK, Wu X, Lindner M, Guryev V, Hiemstra PS, Stolk J, Königshoff M, Gosens R. TGF-β activation impairs fibroblast ability to support adult lung epithelial progenitor cell organoid formation. Am J Physiol Lung Cell Mol Physiol 2019; 317:L14-28. [PMID: 30969812].

57. Montesano R, Orci L. Transforming growth factor beta stimulates collagen-matrix contraction by fibroblasts: implications for wound healing. Proc Natl Acad Sci USA 1988; 85:4894-7. [PMID: 3164478].

58. Kurosaka H, Kurosaka D, Kato K, Mashima Y, Tanaka Y. Transforming growth factor-beta 1 promotes contraction of collagen gel by bovine corneal fibroblasts through differentiation of myofibroblasts. Invest Ophthalmol Vis Sci 1998; 39:699-704. [PMID: 9538875].

59. Lijnen P, Petrov V, Rumilla K, Fagard R. Transforming growth factor-beta 1 promotes contraction of collagen gel by cardiac fibroblasts through their differentiation into myofibroblasts. Methods Find Exp Clin Pharmacol 2003; 25:79-86. [PMID: 12731452].

60. Nakamura Y, Hirano S, Suzuki K, Seki K, Sagara T, Nishida T. Signaling mechanism of TGF-beta1-induced collagen contraction mediated by bovine trabecular meshwork cells. Invest Ophthalmol Vis Sci 2002; 43:3465-72. [PMID: 12407157].

61. Ohmaru-Nakanishi T, Asanoma K, Fujikawa M, Fujita Y, Yagi H, Onoyama I, Hidaka N, Sonoda K, Kato K. Fibrosis in Preeclamptic Placentas Is Associated with Stromal Fibroblasts Activated by the Transforming Growth Factor-β1 Signaling Pathway. Am J Pathol 2018; 188:683-95. [PMID: 29253459].

62. Liu J, Wang Y, Pan Q, Su Y, Zhang Z, Han J, Zhu X, Tang C, Hu D. Wnt/β-catenin pathway forms a negative feedback loop during TGF-β1 induced human normal skin fibroblast-to-myofibroblast transition. J Dermatol Sci 2012; 65:38-49. [PMID: 22041457].

63. Su JY, Yu CC, Peng CY, Liao YW, Hsieh PL, Yang LC, Yu CH, Chou MY. Silencing periostin inhibits myofibroblast trans-differentiation of fibrotic buccal mucosal fibroblasts. J Formos Med Assoc 2021; 120:2010-5. [PMID: 33965260].

64. Bolivar S, Espitia-Corredor JA, Olivares-Silva F, Valenzuela P, Humeres C, Anfossi R, Castro E, Vivar R, Salas-Hernández A, Pardo-Jiménez V, Díaz-Araya G. In cardiac fibroblasts, interferon-beta attenuates differentiation, collagen synthesis, and TGF-β1-induced collagen gel contraction. Cytokine 2021; 138:155359-[PMID: 33160814].

65. Kondo S, Kagami S, Urushihara M, Kitamura A, Shimizu M, Strutz F, Müller GA, Kuroda Y. Transforming growth factor-beta1 stimulates collagen matrix remodeling through increased adhesive and contractive potential by human renal fibroblasts. Biochim Biophys Acta 2004; 1693:91-100. [PMID: 15313011].

66. Vachon PH, Durand J, Beaulieu JF. Basement membrane formation and re-distribution of the beta 1 integrins in a human intestinal co-culture system. Anat Rec 1993; 235:567-76. [PMID: 8465988].

67. Seltana A, Basora N, Beaulieu JF. Intestinal epithelial wound healing assay in an epithelial-mesenchymal co-culture system. Wound Repair Regen 2010; 18:114-22. [PMID: 20082684].

68. de Oliveira RC, Sampaio LP, Shiju TM, Santhiago MR, Wilson SE. Epithelial Basement Membrane Regeneration After PRK-Induced Epithelial-Stromal Injury in Rabbits: Fibrotic Versus Non-fibrotic Corneal Healing. J Refract Surg 2022; 38:50-60. [PMID: 35020537].

69. Yurchenco PD, Patton BL. Developmental and pathogenic mechanisms of basement membrane assembly. Curr Pharm Des 2009; 15:1277-94. [PMID: 19355968].

70. Saikia P, Thangavadivel S, Medeiros CS, Lassance L, de Oliveira RC, Wilson SE. IL-1 and TGF-β Modulation of Epithelial Basement Membrane Components Perlecan and Nidogen Production by Corneal Stromal Cells. Invest Ophthalmol Vis Sci 2018; 59:5589-98. [PMID: 30480706].

Articles are provided courtesy of Emory University and the Zhongshan Ophthalmic Center, Sun Yat-sen University, P.R. China. The print version of this article was created on 20 May 2023. This reflects all typographical corrections and errata to the article through that date. Details of any changes may be found in the online version of the article.